applied sciences

MDPI

Article

Surface Plasmon Resonance Sensor of CO_2 for Indoors and Outdoors

Francisco Pérez-Ocón [1,*], Antonio M. Pozo [1], Jorge Cortina [2] and Ovidio Rabaza [3]

[1] Optics Department, University of Granada, 18071 Granada, Spain; ampmolin@ugr.es
[2] Indra Systems S.A., 28108 Alcobendas, Madrid, Spain; jcortinad@indra.es
[3] Civil Engineering Department, University of Granada, 18071 Granada, Spain; ovidio@ugr.es
* Correspondence: fperez@ugr.es; Tel.: +34-958-241000 (ext. 20011)

Abstract: The ability to detect CO_2 with the smallest possible devices, equipped with alarms and having great precision, is vital for human life, whether indoors or outdoors. It is essential to know if we are being subjected to this gas to establish the level of ventilation in factories, houses, classrooms, etc., and to be protected against viruses or dangerous gas concentrations. Equally, when we are in the countryside, it is useful to be able to evaluate if the greenhouse effect, caused by this gas, is increasing. We propose a surface plasmon resonance (SPR) sensor for the measurement of CO_2 concentrations taking into account that the refractive index of carbon dioxide depends on temperature, humidity, pressure, etc. With our sensor we can measure (in air) in any type of environment and concentration. Our sensor has a resolution of 5.15×10^{-5} RIU and a sensitivity of 19.4 RIU^{-1} for 400 ppm.

Keywords: CO_2 sensor; nanostructure; plasmonic sensors

Citation: Pérez-Ocón, F.; Pozo, A.M.; Cortina, J.; Rabaza, O. Surface Plasmon Resonance Sensor of CO_2 for Indoors and Outdoors. *Appl. Sci.* **2021**, *11*, 6869. https://doi.org/10.3390/app11156869

Academic Editor: Paolo Prosposito

Received: 22 June 2021
Accepted: 23 July 2021
Published: 26 July 2021

1. Introduction

One of the principal problems of CO_2, besides being one of the main causes of the greenhouse effect, is its presence indoors. The variation in the carbon anhidric quantity has fluctuated in a cyclical way since 420,000 years ago and, in the last 100,000 years, at a rate of between 180 ppm and 290 ppm. In the 1950's, the rate of increase was 0.7 ppm per year and in the last 10 years it has increased to 2.1 ppm. Since the end of the industrial revolution, we have reached a global average of 400 ppm, i.e., an increment of 36% in the last century and a half based on data from the Global Monitoring Division of NOAA's Earth System Research Laboratory in Boulder, Colorado [1].

Carbon dioxide affects animals in a harmful way (humans, pets, farm and wild animals, etc.) it affects our homes, workplaces, schools or any other indoor place. CO_2 levels between 2000–5000 ppm produce a diminishing level of concentration, headaches, an increase in cardiac rhythm, somnolence, etc.; however, if levels are increased to 100,000 ppm, humans will lose consciousness and at higher levels of 250,000 ppm, death occurs [2]. The Occupational Safety and Health Administration (OSHA) limits the continuous exposure of CO_2 to 5000 ppm for eight continuous hours, 30,000 ppm in short periods, and 40,000 ppm instantly to cause as little damage as possible [3]. As a quick and first conclusion of the above information it is evident that it is essential to have a sensor which is able to measure both indoors and outdoors without having to modify it in any way.

There are sensors with alarms for gases (CO y CO_2) produced for indoor fires for different concentrations [4], although, there are others which detect only CO_2.

Not all sensors are able to measure all ranges of concentrations, for instance, there is an autoclavable CO_2 sensor which measures concentrations between 0–20%, the average time of the response is 0.7 s, and it needs a recuperation time of approximately 2.0 min [5].

In 2014, Gorma et al. [6] designed and optimized an integrated hybrid surface plasmon biosensor and simulated the results for a medium with refractive indexes between 1.33–1.34. It had a very high sensitivity of around 3000 nm/RIU and a resolution of 3.34×10^{-6} RIU.

There is also an optical spectroscopic sensor based on reflectivity for CO_2 [7] which measures concentrations of between 0.8–44.6%.

In 2016, two sensors were designed for the detection of CO_2. The first one measures concentrations in the range 0–500 ppm with a sensitivity of 6×10^{-9} RIU/ppm and an uncertainty of 20 ppm. It uses the refractometry principle and has the lowest uncertainty of the market [8]. The second one uses a micro-cantiliver structure made of ZnO to detect the CO_2. This sensor is based on the former. The foundation is a crystalline structure of ZnO nanorods. The response to the gas is produced when the resonance frequency of the microcantiliver vibration is increased. It takes approximately 3 min for the gas desorption. This sensor only measures the presence/no presence of CO_2 [9].

As for planar waveguide optical sensors, there is one made of planar waveguides with a cladding made of extract of Alstonia Scholaris leaves. It takes 4–5 s for the measurement and needs a period of about 5 s to measure again. The range of measurement is 0–62,500 ppm and it has a lifetime of 25–30 days. It is not able to measure with humidity above 70% [10].

Another sensor is made of an ellipsoidal planar waveguide with which it is possible study the dependence of the concentration and temperature. It has been demonstrated that an increase of 80 °C produces a standard deviation of 5%. This sensor has a range of 0–3000 ppm [11].

An optical fiber sensor has been developed for detecting concentrations of CO_2 in oceans. It requires a stabilization time of 5 min and has a sensitivity of 0.2371 RIU^{-1} [12].

Another optical fiber sensor is based on fluorescence. It works in the mid-infrared range and considers a minimum of CO_2 in 400 ppm (atmospheric average). The range is 500–3000 ppm and the resolution is 5% [13].

The next sensor is based on the absorption of transmitted light for an optical fiber. The response time varies between 20 s and 100 s, depending on the thickness of the layer [14].

Based on the principle of the Fabry-Perot interferometer (with optical fiber), a CO_2 sensor was constructed to measure concentrations of 0–700 ppm [15].

There is another optical fiber sensor which measures a range of 0–75% of CO_2 and has a dynamic response of 6.1 min and 8 min when the up time is 2.12 min and the down time is 2.95 min [16].

In 2009, the first sensor plasmon resonance (SPR) was introduced and it operated in the mid-infrared range to detect CO_2. It is based on the model of Kretschmann, with a glass prism of CaF_2 and a layer of Ti and another of Au. The sensitivity is so far the highest of all the CO_2 sensors, 10^{-5} RIU^{-1} [17].

Another SPR with a mixture of polymer is able to trap CO_2 in a reversible way. It works with a wavelength of 640 nm and measures CO_2 dissolved in synthetic air. The limit of concentration is 10 ppm [18].

In 2015, Nuryadi et al. manufactured a gas sensor with the Kretschmann configuration, modifying the hemiprism, and after the layer of Au, they used a ZnO layer in a cylindrical way where the CO_2 circulates. This is a sensor of presence; it is not able to measure quantities [19].

It is interesting to mention some plasmonic optical fiber sensors as well, since they are currently attracting a large amount of research interest for the detection of gases [20,21].

Table 1 summarizes the key characteristics of the studied sensors so that they can be compared easily and quickly. The number in brackets corresponds to the reference number of the paper.

Table 1. Summary table with the essential characteristics of the sensors studied.

Indoor	Outdoor	Multigas	Only CO_2	Wide Dynamic Range	Short Dynamic Range
[4]	[12,19]	[20,21]	[5–13]	[7,11,16]	[5,6,8,13,15,18]
Waveguide/Optical fiber sensor	**Plasmonic sensor**	**Others**	**Instant response time**	**Fast response time**	**Slow response time**
[10–16,20,21]	[6,17–19]	[5,7–9]	[6,17–19]	[5,10]	[9,14,16]
High resolution	**Low resolution**	**High sensitivity**	**Low sensitivity**		
[17]	[13]	[8,17,20]	[12]		

In view of all the limitations of the sensors described above, we propose a CO_2 sensor able to detect very high, high, normal, low and very low concentrations which could work both indoors and outdoors without any modification of the structure, wavelength, etc.

2. Design of the Plasmonic Sensor

The operational principle is based on SPR [22,23].

Figure 1 shows a diagram of the sensor for the measurement of the concentration of CO_2. The experimental set up is schematically illustrated in Figure 1.

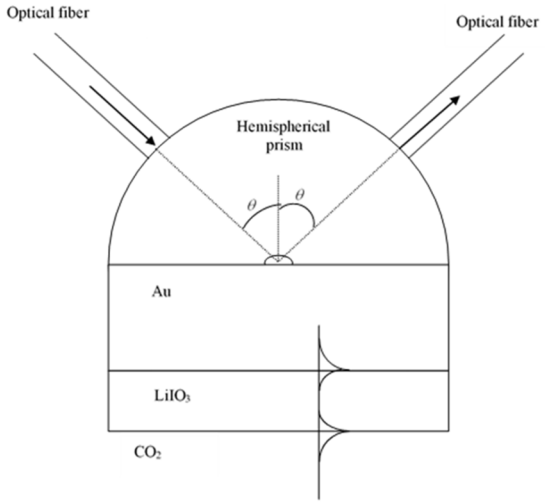

Figure 1. Diagram of the plasmonic sensor. On the left of the hemispherical prism, the optical fiber transports the incident radiation and, on the right, another optical fiber collects the reflected radiation. The SPR are also shown propagating through the $LiIO_3$-Au and Au-medium interfaces.

It can be considered that the standard air is a mixture of 78% of N_2, 21% of O_2 and 1% of Ar, CO_2 (0.04%) and H_2O.

As we can measure the concentration of CO_2 both indoors and outdoors, we have to know the variation of the refractive index of the carbon dioxide with atmospheric pressure, temperature, height above the sea level, concentration, etc.

A slight variation in humidity of 2 mb may cause a variation of 14% in relative humidity. This affects the eighth-decimal place of the refractive index of CO_2 in concentrations of 200–400 ppm.

The difference between the refractive indexes of the CO_2 when the atmospheric pressure varies from 0.5 atm to 1 atm is 1.00025 to 1.0005, respectively, if we consider an atmospheric pressure in the middle, 0.74 atm, the refractive index is 1.000375 [24].

From the Edlén equations, we can calculate the dispersion of the refractive index of the carbonic anhydride for dry air, 1 atm, 15 °C and 300 ppm in volume. This variation is around 10–8 from 200 nm up to the infrared.

Another parameter which provokes variations in the refractive index is the temperature. For 1 atm and 20 °C, (n − 1) = 0.000271786 (a variation to the fourth decimal place which we have to take into account). The variation in the refractive index with the water vapour can be calculated with the correction of Birch and Downs [25].

The effects of other gases, such as Ar, N_2 and O_2, have no effect on the change in the refractive index of carbon dioxide.

Due to all of the above, our sensor would be able to measure the refractive index for different concentrations of CO_2. As the variation of the refractive index with pressure is very great, these sensors have to be designed taking into account the height above sea level where they are going to be used.

The hemispheric prism is made of glass SUMITA (CaFK) (n = 1.4333) [26]. The dielectric layer is lithium iodate ($LiIO_3$) with a thickness of 37.26 nm, and the refractive index is 1.8807 [27]. The Au layer has a thickness of 51.48 nm and a refractive index of (n = 0.12517 + 3.3326i) [28].

The hemispherical prism has a radius of 1 cm.

The laser used is a continuous emission (to minimize consumption), with polarization *p* and a wavelength of 632.8 nm. It strikes the spherical part of the hemiprism with a normal incidence. The light is conducted from the laser to the prism by means of an optical fiber and its endface is glued to the surface of the hemiprism. The incidence angle, compared to the normal, in the $LiIO_3$ is θ (greater than the critical angle) (see Figure 1). The reflected light in the interface prism-$LiIO_3$ reaches the other optical fiber and it transports the light to the photodetector.

When the laser strikes the interface prism-Au with an angle greater than the critical angle, an evanescent wave is produced on the surface. If both the thickness of the layers and the geometry of the sensor are adequate, it is possible to excite two superficial plasmons propagating through the surfaces.

The sensor we have designed is based on intensity interrogation. This allows us to differentiate the refractive index of the medium with which our sensor is in contact. The principal advantage this sensor offers, compared to the others which work with angle interrogation, is that ours has no mobile parts, no friction hysteresis and backlash are eliminated, the response time is minimized and we save energy. For the theoretical model of surface plasmon resonance reflectance, the transfer matrix method was used to solve the Fresnel equations for the multilayer [29,30] with the WinSpall software package.

This sensor has been designed to differentiate the quantity of CO_2 in ppm in air. For a given angle of incidence θ, we obtain different reflectances for different concentrations of carbon dioxide. These values are sufficiently different from one another to effectively differentiate the reflectance with the photodetector in the endface of the optical fiber.

We know that the concentration of carbon dioxide is not distributed homogeneously all over the planet. Our sensor is able to measure the concentration of CO_2 each instant, it can measure the concentration at the moment of the installation to know the level of CO_2 and decide from what amount of carbon dioxide the alarm signal will be given, either indoors or outdoors. We do not need a sensor of reference.

3. Results and Discussion

Figure 2 shows the graphic for different concentrations of CO_2 for an incidence angle close to 84° and, as for example, for 1000 m above sea level.

Depending on the reflectance in the photodetector, we can detect the concentration of CO_2 in real time. It is essential to know the relative humidity and pressure of the air to know the refractive index of the mixture of the air (therefore the CO_2 concentration) so that the plasmonic sensor can accurately measure the refractive index and then know the CO_2 concentration.

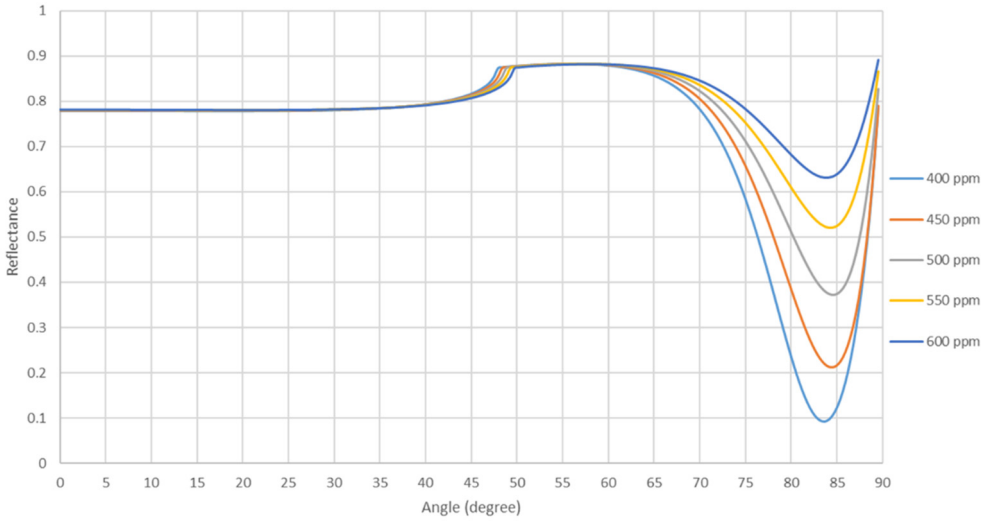

Figure 2. Reflectance curves as a function of the angle of incidence of the light in the prism and different concentration of CO_2. The height above sea level is 1000 m. The sensor works with an incidence angle of 83.67°.

The sensitivity of our sensor can be calculated from the change in reflectance per unit of change in refractive index (see Table 2 with more detail and data).

Table 2. The sensitivity and resolution values of the sensor as a function of altitude and gas concentration change.

Altitude (m)	Sensitivity (RIU^{-1}) and Resolution (RIU)	400–450 ppm	450–500 ppm	500–550 ppm	550–600 ppm
0	Sensitivity	17.18	22.07	19.53	14.71
	Resolution $\times 10^{-5}$	5.80	4.55	5.10	6.80
500	Sensitivity	13.39	20.54	20.76	17.28
	Resolution $\times 10^{-5}$	7.45	4.85	4.80	5.80
1000	Sensitivity	19.37	24.89	22.03	16.59
	Resolution $\times 10^{-5}$	5.15	4.02	4.54	6.05
1500	Sensitivity	7.51	16.54	20.65	20.16
	Resolution $\times 10^{-4}$	1.33	0.61	0.49	0.50
2000	Sensitivity	6.01	14.75	19.70	20.45
	Resolution $\times 10^{-4}$	1.67	0.68	0.51	0.49
2500	Sensitivity	6.68	14.37	18.98	20.12
	Resolution $\times 10^{-4}$	1.50	0.70	0.53	0.50
3000	Sensitivity	5.09	12.53	17.68	19.82
	Resolution $\times 10^{-4}$	1.97	0.80	0.57	0.51
3500	Sensitivity	3.88	10.91	16.28	19.16
	Resolution $\times 10^{-4}$	2.58	0.92	0.62	0.52
4000	Sensitivity	3.02	9.56	14.92	18.28
	Resolution $\times 10^{-4}$	3.31	1.05	0.67	0.55
4500	Sensitivity	2.59	8.62	13.79	17.37
	Resolution $\times 10^{-4}$	3.87	1.16	0.73	0.58
5000	Sensitivity	2.36	7.89	12.79	16.43
	Resolution $\times 10^{-4}$	4.24	1.27	0.78	0.61
5500	Sensitivity	2.41	7.47	12.04	15.62
	Resolution $\times 10^{-4}$	4.16	1.34	0.83	0.64

The sensor resolution depends upon the accuracy with which the monitored SPR parameter can be determined by the specific sensing device and, as such, is limited by sensor-system noise [31]. To calculate the resolution of the sensor, we divide the accuracy of the photodetector by its sensitivity. Considering an accuracy of 0.1% in the signal registered by the photodetector [32,33], we achieve resolutions of 5.15×10^{-5} RIU, 4.02×10^{-5} RIU, 4.54×10^{-5} RIU and 6.05×10^{-5} RIU for concentrations of 400 ppm, 450 ppm, 500 ppm,

550 ppm and 600 ppm respectively. This resolution is more than adequate to accurately measure the CO_2 concentration. With a variation of the fifth decimal place, we can assure that the measurements of the refractive indexes are reliable, taking into account that the variations of the refractive indexes due to pressure, temperature, humidity and concentration are to the third decimal place. The sensor of Herminjard et al. [17] has a resolution similar to ours, but uses infrared while our laser is in the range of the visible; it is also cheaper and more commercially viable.

The effect of the thickness of the Au and $LiIO_3$ layers and the wavelength of the laser influences the reflectance, sensitivity and the distance between the curves of each of the concentrations.

The photodetector, which is at the end of the output optical fiber, has a reference signal. This reference is the laser that has passed through all the optical media in the total absence of CO_2. We will therefore have the response of the photodetector at a concentration of 0 ppm.

The refractive index of CO_2 increases concomitantly with increasing concentration. As the concentration of CO_2 in the medium increases, the reflected radiation that is injected into the output optical fiber and reaches the photodetector will decrease. When the refractive index increases, the reflectivity decreases and we will get closer to the formation of the SPR [22,23]. By comparing this photodetector output signal with the 0 ppm, we are able to calculate the reflectivity. Once the reflectivity is known, as we see in the curves in Figure 2, we are able to know the CO_2 concentration at each moment.

The sensor of Mi et al. [8] has a better resolution than ours, however, the range is only 0–500 ppm and our sensor has more range than the others [5,8,11,15,16].

The sensor measures continuously and there is no waiting time between measurements as in the others [5,9,10,12,14,16,34].

The sensitivity of our sensor is greater than sensors which have satellites NOAA and Aqua Terra [4,12,34,35] and the plasmonic sensors [8].

Our sensor is smaller than the UV Strip Resistive Thick GEM (S-RETGEM) [8] and measures concentrations of carbon dioxide instead of measuring presence of this gas [9,19] and is able to measure with any value of the humidity unlike the sensor of Vijayan et al. [10].

The sensor of Gorma et al. [6] had a very high sensitivity, of around 3000 nm/RIU and a resolution of 3.34×10^{-6} RIU, better results than ours, however, this design works in wavelength interrogation, so we were unable to compare.

If we are measuring concentrations of CO_2 in a controlled ambient, it is not necessary to take into account the variations of humidity, temperature or pressure because these are minimum, therefore the results obtained from the sensor can be used without having to take into account the Edlén or modified Birch and Downs equations. Therefore, our sensor could measure concentrations of CO_2 indoors (houses, factories, motors, etc.) without applying the Edlén and Birch and Downs equations.

If we are measuring outdoor CO_2 concentrations, as the variations of the variables are not controlled, the changes in the refractive indices will vary with humidity, pressure, temperature, etc. After using the sensor, very simple software modifies the measured refractive indices based on these parameters and will give us the real concentration of the gas based on the Birch and Downs equations.

4. Conclusions

We have designed an SPR sensor for the detection of concentrations of CO_2 which works both indoors and outdoors. The sensor has a sensitivity of almost 25 RIU^{-1} and a resolution of 5.15×10^{-5} RIU. It could have better sensitivity if the ambient conditions are known because the refractive index of this gas depends on pressure, temperature, humidity and concentration. This is an improvement compared to other SPR sensors designed to work indoors and outdoors.

Measurements are made continuously and no time is needed to achieve the measurement, and there is no time lapse between measurements.

Today, it is vital to ventilate closed spaces to avoid the spread of COVID-19. We cannot be sure if the ventilation time is correct or if a building is well ventilated because we do not have sensors that measure the presence of the virus in the air, but we can indirectly know the correct ventilation of the rooms from the measurement of CO_2 expelled by humans, so we can know the distribution of this residual CO_2. By placing our sensors in the right places, we can know if the ventilation is adequate and, therefore, we will know if the ventilation time is adequate. As our sensor is so tiny, many can be placed and at any point in a room to see the data of concentration of CO_2 in real time.

The overall system can be connected to a 5G module to send data to a remote point and there is an alarm if the data is superior and potentially damaging for health, the environment, etc.

Finally, it is not necessary to carry out periodic calibrations.

Author Contributions: Conceptualization, A.M.P. and F.P.-O.; methodology, J.C.; software, J.C. and O.R.; validation, A.M.P. and F.P.-O.; formal analysis, J.C.; investigation, A.M.P., F.P.-O., J.C. and O.R.; resources, A.M.P., F.P.-O., J.C. and O.R.; data curation, J.C. and O.R.; writing—original draft preparation, F.P.-O.; writing—review and editing, A.M.P., J.C. and O.R.; visualization, A.M.P., F.P.-O., J.C. and O.R.; supervision, A.M.P. and F.P.-O. All authors have read and agreed to the published version of the manuscript.

Funding: This research received no external funding.

Institutional Review Board Statement: Not applicable.

Informed Consent Statement: Not applicable.

Data Availability Statement: Not applicable.

Acknowledgments: The authors wish to thank Angela L. Tate, a native English speaker and expert in translations of scientific papers, for her assistance with the English version.

Conflicts of Interest: The authors declare no conflict of interest.

References

1. Butler, J.H. CO_2 at NOAA's Mauna Loa Observatory Reaches New Milestone: Tops 400 ppm, Global Monitoring Division—ESRL-GMD. Available online: http://www.esrl.noaa.gov/gmd/ccgg/trends/weekly.html (accessed on 24 June 2021).
2. Satish, U.; Mendell, M.J.; Shekhar, K.; Hotchi, T.; Sullivan, D.; Streufert, S.; Fisk, W.J. Is CO_2 an Indoor Pollutant? Direct Effects of Low-to-Moderate CO_2 Concentrations on Human Decision-Making Performance. *Environ. Health Perspect.* **2012**, *120*, 1671–1677. [CrossRef]
3. Chemical Sampling Information | Carbon Dioxide | Occupational Safety and Health Administration. 2018. Available online: https://www.osha.gov/dts/chemicalsampling/data/ (accessed on 20 June 2021).
4. Chen, S.J.; Hovde, D.C.; Peterson, K.A.; Marshall, A.W. Fire Detection using Smoke and Gas Sensors. *Fire Safety. J.* **2007**, *42*, 507–515. [CrossRef]
5. Ge, X.D.; Kostov, Y.; Rao, G. High-stability Non-invasive Autoclavable Naked Optical CO_2 Sensor. *Biosens. Bioelectron.* **2003**, *18*, 857–865. [CrossRef]
6. Gorman, T.; Haxha, S. Design and Optimization of Integrated Hybrid Surface Plasmon Biosensor. *Opt. Commun.* **2014**, *325*, 175–178. [CrossRef]
7. Salim, M.R.; Yaacob, M.; Ibrahim, M.H.; Azmi, A.I.; Ngajikin, N.H.; Dooly, G.; Lewis, E. An Optical Spectroscopic Based Reflective Sensor for CO_2 Measurement with Signal to Noise Ratio Improvement. *J. Optoelectron. Adv. Mater.* **2015**, *17*, 519–525.
8. Mi, J.G.C.; Horvath, C.; Aktary, M.; Van, V. Silicon Microring Refractometric Sensor for Atmospheric CO_2 gas Monitoring. *Opt. Express* **2016**, *25*, 1773–1780. [CrossRef]
9. Nuryadi, R.; Aprilia, L.; Gustiono, D. CO Gas Response of ZnO Nanostructures using Microcantilever in Dynamic Mode Operation. In Proceedings of the 7th IEEE International Nanoelectronics Conference, Chengdu, China, 9–11 May 2016. Available online: https://ieeexplore.ieee.org/stamp/stamp.jsp?tp=&arnumber=7589337 (accessed on 20 June 2021).
10. Vijayan, A.; Fuke, M.V.; Karekar, R.N.; Aiyer, R.C. Planar Optical Waveguide Evanescent Wave CO_2 Sensor based on a Clad of Alstonia Scholaris Leaf Extract. *IEEE Sens. J.* **2009**, *9*, 13–19. [CrossRef]
11. Yi, S. Temperature Compensation Methods of Nondispersive Infrared CO_2 gas Sensor with Dual Ellipsoidal Optical Waveguide. *Sensors Mater.* **2017**, *29*, 243–252. [CrossRef]
12. Bao, B.; Melo, L.; Davies, B.; Fadaei, H.; Sinton, D.; Wild, P. Detecting Supercritical CO_2 in Brine at Sequestration Pressure with an Optical Fiber Sensor. *Environ. Sci. Technol.* **2013**, *47*, 306–313. [CrossRef]

13. Starecki, F.; Charpentier, F.; Doualan, J.L.; Quetel, L.; Michel, K.; Chahal, R.; Troles, J.; Bureau, B.; Braud, A.; Camy, P.; et al. Mid-IR Optical Sensor for CO_2 Detection based on Fluorescence Absorbance of Dy^{3+}: $Ga_5Ge_{20}Sb_{10}S_{65}$ fibers. *Sens. Actuators B Chem.* **2015**, *207*, 518–525. [CrossRef]
14. Wysokinski, K.; Napierała, M.; Stanczyk, T.; Lipinski, S.; Nasiłowski, T. Study on The Sensing Coating of The Optical Fibre CO_2 Sensor. *Sensors* **2015**, *15*, 31888–31903. [CrossRef]
15. Ma, W.W.; Xing, J.X.; Wang, R.H.; Rong, Q.Z.; Zhang, W.L.; Li, Y.C.; Zhang, J.Y.; Qiao, X.G. Optical Fiber Fabry–Perot Interferometric CO_2 gas Sensor using Guanidine Derivative Polymer Functionalized Layer. *IEEE Sens. J.* **2018**, *18*, 1924–1929. [CrossRef]
16. Wu, J.S.; Yin, M.J.; Seefeldt, K.; Dani, A.; Guterman, R.; Yuan, J.Y.; Zhang, A.P.; Tam, H.Y. In Situ Mu-printed Optical Fiber-tip CO_2 Sensor using a Photocross Linkable Poly (ionic liquid). *Sens. Actuators B Chem.* **2018**, *259*, 833–839. [CrossRef]
17. Herminjard, S.; Sirigu, L.; Herzig, H.P.; Studemann, E.; Crottini, A.; Pellaux, J.P.; Gresch, T.; Fischer, M.; Faist, J. Surface Plasmon Resonance Sensor showing Enhanced Sensitivity for CO_2 Detection in the Mid-infrared Range. *Opt. Express* **2009**, *5*, 293–303. [CrossRef]
18. Lang, T.; Hirsch, T.; Fenzl, C.; Brandl, F.; Wolfbeis, O.S. Surface Plasmon Resonance Sensor for Dissolved and Gaseous Carbon Dioxide. *Anal. Chem.* **2012**, *84*, 9085–9088. [CrossRef]
19. Nuryadi, R.; Mayasari, R.D.; Aprilia, L.; Yuliarto, B. Fabrication of ZnO/Au/prism-based Surface Plasmon Resonance Device for Gas Detection. Presented at International Conference on Quality in Research (QiR), Lombok, Indonesia, 10–13 August 2015. [CrossRef]
20. González-Vila, A.; Ioannou, A.; Loyez, M.; Debliquy, M.; Lahem, D.; Caucheteur, C. Surface Plasmon Resonance Sensing in Gaseous Media with Optical Fiber Gratings. *Opt. Letters* **2018**, *43*, 2308–2311. [CrossRef]
21. Yao, Q.F.; Ren, G.H.; Xu, K.; Zhu, L.; Khan, H.; Mohiuddin, M.; Khan, M.W.; Zhang, B.Y.; Jannat, A.; Haque, F.; et al. 2D Plasmonic Tungsten Oxide Enabled Ultrasensitive Fiber Optics Gas Sensor. *Adv. Opt. Mater.* **2019**, *7*. [CrossRef]
22. Pozo, A.M.; Pérez-Ocón, F.; Rabaza, O. A Continuous Liquid-level Sensor for Fuel Tanks based on Surface Plasmon Resonance. *Sensors* **2016**, *16*, 724. [CrossRef]
23. Pérez-Ocón, F.; Pozo, A.M.; Serrano, J.M.; Rabaza, O. Continuous Measurement with Three-in-one Plasmon Sensor in Sucrose Solutions. *IEEE Sens. J.* **2020**. (In Press) [CrossRef]
24. Sang, B.H.; Jeon, T.I. Pressure-dependent Refractive Indices of Gases by THz Time-domain Spectroscopy. *Opt. Express* **2016**, *24*, 29040–29047. [CrossRef]
25. Birch, K.P.; Downs, M.J. The results of a Comparison between Calculated and Measured Values of The Refractive Index of Air. *J. Phys. E Sci. Instrum.* **1988**, *21*, 694–695. [CrossRef]
26. Optical Glass | Sumita Optical Glass. Available online: http://www.sumita-opt.co.jp/en/products/optical (accessed on 20 June 2021).
27. Choy, M.M.; Byer, R.L. Accurate Second-order Susceptibility Measurements of Visible and Infrared Nonlinear Crystals. *Phys. Rev. B* **1976**, *14*, 693–706. [CrossRef]
28. Babar, S.; Weaver, J.H. Optical Constants of Cu, Ag, and Au Revisited. *Appl. Opt.* **2015**, *54*, 477–481. [CrossRef]
29. Heavens, OS Thin Films Optics. *Optical Properties of Thin Solid Films*; Dover Books on Physics: New York, NY, USA, 2011; pp. 45–96.
30. Ohta, K.; Ishida, H. Matrix Formalism for Calculation of Electric Field Intensity of Light in Stratified Multilayered Films. *Appl. Opt.* **1990**, *29*, 1952–1959. [CrossRef]
31. Homola, J.; Yee, S.S.; Gauglitz, G. Surface Plasmon Resonance Sensors: Review. *Sens. Actuators B Chem.* **1999**, *54*, 3–15. [CrossRef]
32. Ronot-Trioli, C.; Trouillet, A.; Veillas, C.; Gagnaire, H. Monochromatic Excitation of Surface Plasmon Resonance in an Optical Fibre Refractive-index Sensor. *Sens. Actuators A Phys.* **1996**, *54*, 589–593. [CrossRef]
33. Derbel, F. Performance Improvement of Fire Detectors by Means of Gas Sensors and Neural Networks. *Fire Safety, J.* **2004**, *39*, 383–398. [CrossRef]
34. Fraser, R.H.; Li, Z.; Cihlar, J. Hotspot and NDVI Differencing Synergy (HANDS): A new Technique for Burned Area Mapping Over Boreal Forest. *Remote Sens. Environ.* **2000**, *74*, 362–376. [CrossRef]
35. Mu, M.; Randerson, J.T.; Van der Werf, G.R.; Giglio, L.; Kasibhatla, P.; Morton, D.; Collatz, G.J.; De Fries, R.S.; Hyer, E.J.; Prins, E.M.; et al. Daily and 3-hourly Variability in Global Fire Emissions and Consequences for Atmospheric Model Predictions of Carbon Monoxide. *J. Geophys. Res.* **2011**, *116*, 1–19. [CrossRef]